

A LOW PHASE-NOISE PIERCE OSCILLATOR USING A PIEZOELECTRIC-ON-SILICA MICROMECHANICAL RESONATOR

Z. Z. Wu¹, V. A. Thakar², A. Peczalski¹, and M. Rais-Zadeh^{1,2}

¹Electrical Engineering Department, University of Michigan, Ann Arbor, MI 48109, USA

²Mechanical Engineering Department, University of Michigan, Ann Arbor, MI 48109, USA

ABSTRACT

In this paper, we report on a low phase-noise 4.9 MHz oscillator using a fused silica micro-mechanical resonator. The resonator is implemented using a piezoelectric -on-silica structure, achieving high quality factor ($Q \sim 15,860$) and low motional impedance ($R_m \sim 360 \Omega$). By interfacing the resonator to a CMOS amplifier, an oscillator phase noise of -138 dBc/Hz at 1 kHz, -154 dBc/Hz at 10 kHz, and -155 dBc/Hz at far-from-carrier offset frequencies has been achieved at a low-supply voltage. Vibration tests on the oscillator indicate an acceleration sensitivity of less than 4 ppb/g. The frequency tuning properties of the silica oscillator are also characterized for compensating frequency variations due to environmental effects.

KEYWORDS

MEMS, micromechanical, resonator, oscillator, phase noise, piezoelectric tuning, acceleration sensitivity.

INTRODUCTION

Microelectromechanical (MEMS) oscillators have shown great potential in realizing miniaturized and integrated timing references. In the past, efforts have been focused on developing silicon-based micromechanical oscillators and improving their performance, including phase noise, temperature stability, long-term aging, etc., in order to replace bulky quartz crystal oscillators [1-5]. Several silicon MEMS oscillators with low jitter and phase noise have been demonstrated that satisfy GSM specifications, pushing MEMS technology towards high-end timing applications [1-4]. The stability of MEMS oscillators can be further improved using a low-power oven [6]. Oven-controlled MEMS can realize ultra-stable timing references, leading to orders of magnitude reduction in size and power consumption compared to conventional oven-controlled crystal oscillators (OCXOs) used in more demanding applications.

Fused silica is an alternative material that has a low acoustic loss and low thermal conductivity [7]. The low thermal conductivity of fused silica results in low thermoelastic damping (TED) [7]. Silica resonators and resonant sensors can thus outperform silicon-based devices at low frequencies where TED is a limiting factor. In addition, the low thermal conductivity and the small thermal expansion coefficient make silica ideal as the packaging material, enabling all-silica packaged MEMS that can be thermally isolated from external environment and oven-controlled at low powers.

We have previously demonstrated a fused silica resonator that exhibits a high- Q , low motional impedance, and good power handling capability [8]. In this paper, we report on a MEMS oscillator by interfacing a fused silica

micro-mechanical resonator to a 180 nm CMOS circuit and characterize its performance in terms of frequency tuning, acceleration sensitivity, and phase noise. This is the first demonstration of a fused silica micro-electromechanical oscillator.

PIEZO-ON-SILICA RESONATOR

The silica resonator comprises of two vibrating rings mechanically coupled through a center beam, as shown Fig. 1. The target vibration mode is the in-plane coupled radial extensional mode (breathing mode). This mode can be effectively transduced using piezoelectric transduction. For this purpose, a piezoelectric stack consisting of the bottom and top electrodes and a thin film aluminum nitride (AlN) layer is deposited on the silica resonator area. Fig. 2 shows a scanning electron microscope (SEM) image of a fabricated silica resonator which is employed in the MEMS oscillator of this work. The measured frequency response of the breathing mode is plotted in Fig. 3. The resonance frequency is at 4.9 MHz with a measured Q of 15,860 and an insertion loss of 14.3 dB (motional impedance of $\sim 360 \Omega$). By changing the source power in S-parameter measurements, the power handling of the resonator is characterized, as shown in Fig. 4. The silica resonator is stable up to a source power of +5 dBm, although non-linearity starts to show at a source power of 0 dBm.

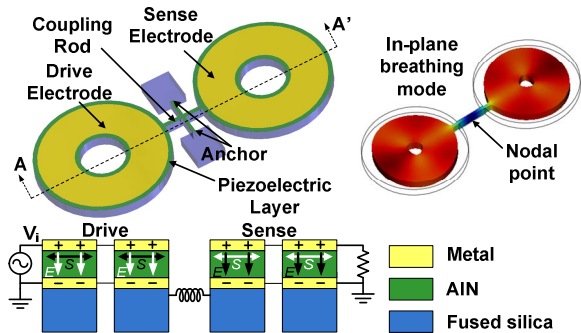


Figure 1: (Top) 3D model and vibration mode shape of the silica resonator. (Bottom) piezoelectric actuation diagram.

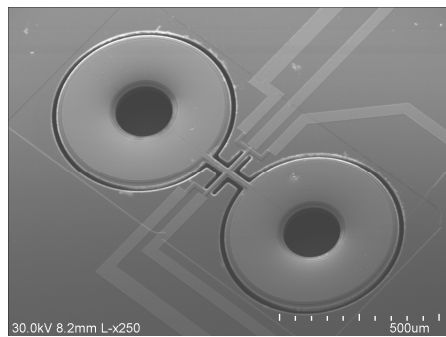


Figure 2: SEM image of the fabricated silica resonator.

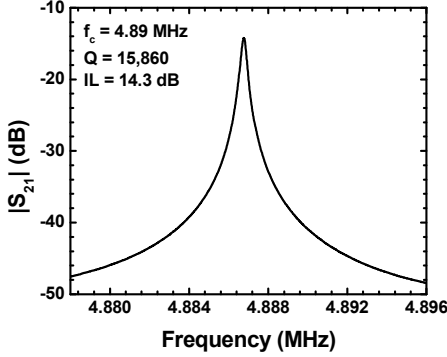


Figure 3: S-parameter response of the in-plane radial extensional mode at 4.9 MHz.

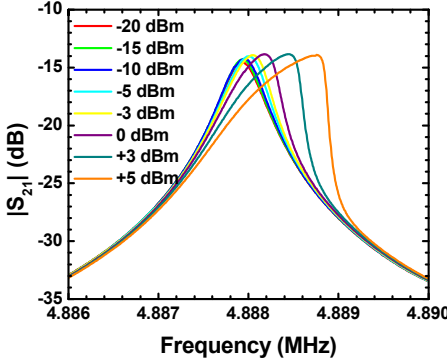


Figure 4: S-parameter responses of the 4.9 MHz mode at various source power levels.

SILICA MEMS OSCILLATOR

Leeson's model [9] describe the oscillator phase noise at offset frequency (Δf) from the oscillator's carrier frequency (f_0) as

$$L\{\Delta f\} = 10 \log \left\{ \frac{k_b T F}{P_{sig}} \left(\frac{1}{4Q_L^2} \left(\frac{f_0}{\Delta f} \right)^2 + 1 \right) \right\}, \quad (1)$$

where k_b is the Boltzmann constant, T is the absolute temperature in Kelvin, F is the noise factor of the sustaining amplifier, Q_L is the loaded quality factor of the resonator, and P_{sig} is the oscillator carrier power. The high- Q of the 4.9 MHz silica resonator helps obtain a high Q_L , which shapes the close-in-carrier phase noise. Low motional impedance and good power handling of the silica resonator ensures that sufficiently high P_{sig} can be obtained when a relatively low voltage swing is driving the silica resonator. This in turn results in a low phase noise at far-from-carrier.

A Pierce-type oscillator is designed using 180 nm 1P6M CMOS technology (Fig. 5), and the CMOS circuit is interfaced to the silica resonator at the board level. Due to the low motional impedance of silica resonator, a self-biased CMOS inverter provides sufficient gain as an oscillator sustaining amplifier. Such oscillator has a minimum number of transistors to help reduce circuit noise factor. The Peirce oscillator is also robust against spurious modes present in the resonator. As can be observed from the wideband frequency response of the silica resonator in Fig. 6, there exist an out-of-phase radial extensional mode and other spurious modes in addition to the desired in-phase breathing mode. The value of capacitors C_{p1} and C_{p2} can be properly sized such that the oscillator is locked

into the 4.9 MHz in-phase breathing mode, which has a high $f \times Q$ product. C_{p1} and C_{p2} can also absorb chip and package parasitic capacitances. The output voltage that drives the silica resonator swings almost rail-to-rail. The supply voltage (V_{DD}) of the circuit can be tuned to control the power driving the resonator.

The phase noise performance is measured using an Agilent E5500 system, and DC voltage is supplied using Agilent E3612A. At a low supply voltage (V_{DD}) of 1 V (a bias current of $\sim 120 \mu\text{A}$ on NMOS and PMOS), the silica oscillator shows a phase noise of -138 dBc/Hz at 1 kHz offset, -154 dBc/Hz at 10 Hz offset, and -155 dBc/Hz at far-from-carrier (Fig. 7). The close-in-carrier phase noise meets the stringent GSM specifications [1] and is comparable to that of the reported silicon-based MEMS oscillators (Table 1). While the use of piezoelectric transduction eliminates the noise from the DC bias applied to the resonator itself, the phase noise shows spurs induced from the Agilent E3612A power supply (Fig. 7). Such supply noise can be reduced using a voltage regulator.

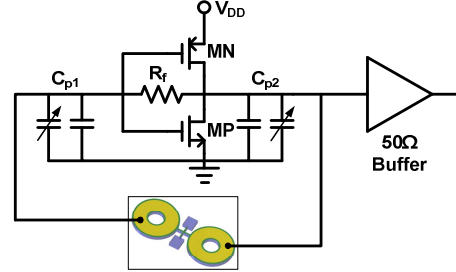


Figure 5: Schematic of the MEMS Pierce oscillator.

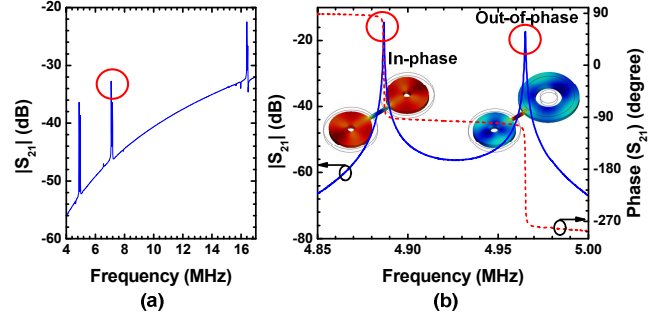


Figure 6: (Left) The measured wideband frequency response of the piezoelectric-on-silica resonator. (Right) Highlighted response near 4.9 MHz, showing the in-phase main mode and another out-of-phase vibration mode.

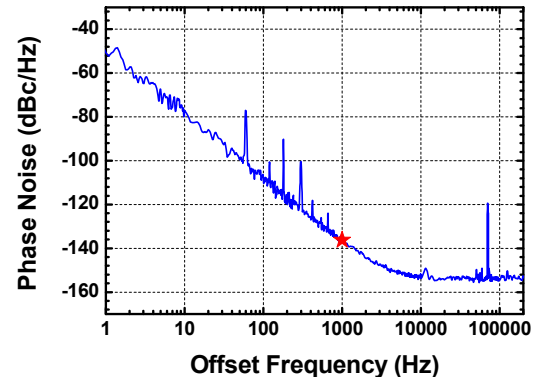


Figure 7: Measured phase noise of the silica MEMS oscillator at a low supply voltage (V_{DD}) of 1 V. The star symbol marks the GSM close-in-carrier specification.

Table 1: Performance comparison of the silica MEMS oscillator with reported silicon MEMS oscillators.

Oscillator	Resonator	Phase Noise (dBc/Hz)
60 MHz [1]	Silicon	-123 @ 1 KHz; -136 floor
145MHz [2]	Silicon	-111 @ 1 KHz; -133 floor
496 MHz [3]	AlN-on-Si	-92 @ 1 KHz; -147 floor
6 MHz [4]	Silicon	-112 @ 1 KHz; -135 floor
This work 4.9 MHz	AlN-on-silica	-138 @ 1 kHz; -154 @ 10 KHz; -155 floor

VIBRATION SENSITIVITY

Timing references are frequently used in applications, such as navigation systems, radars, and mobile devices, where external vibrations are significant. Vibration causes a shift in the center frequency of the resonator and degrades the phase noise of the oscillator. In this work, the use of piezoelectric transduction eliminates the impact of vibration on electrical stiffness, which can dominate the frequency drift in capacitive MEMS resonators. Instead, the frequency shift of silica resonator is mainly due to the mechanical stress induced from vibration. Quartz oscillators can experience similar effects [10], with a typical frequency shift of $10^{-12}/g$ for precision SC-cut quartz to greater than $10^{-7}/g$ for low-cost AT-cut quartz. As the silica micro-resonator has very small mass compared to quartz resonator, the effect of vibration is expected to be less significant. Using COMSOL FEM software, the vibration sensitivity of the silica resonator has been simulated to be $\Delta f/f_0 < 10^{-12} \text{ g}^{-1}$ in all directions (Fig. 8).

The vibration sensitivity is difficult to measure by directly capturing the small shift of resonance peak in the S-parameter response. Instead, as vibration modulates the oscillator output signal and hence excites sideband peaks in the oscillator output spectrum; the vibration sensitivity of the oscillator can be extracted from the power of the sideband peaks [10]. The vibration-induced frequency shift Δf_{vib} for a resonator is often expressed as

$$\Delta f_{vib} / f_0 = \Gamma \cdot \mathbf{a}, \quad (2)$$

where f_0 is the resonance frequency, \mathbf{a} is the vector acceleration, and Γ is the vector vibration sensitivity.

With an external vibration at frequency f_v , the power of the sideband peak excited by vibration can be expressed as

$$L(f_v) = 20 \log \left[(\Gamma \cdot \mathbf{a}) \frac{f_0}{2f_v} \right]. \quad (3)$$

To measure the vibration sensitivity, the silica MEMS oscillator is mounted in a custom-made vacuum chamber. The vacuum chamber is then firmly mounted on a vibration stage while the MEMS oscillator is running. An Agilent E5500 phase noise measurement tool is used to capture the sideband peaks due to external vibration. The sideband peak excited by vibration appears as a spur in the phase noise measurement tool, which is captured as the output power of the spur (in dBm) instead of phase noise power density (dBc/Hz). The sensitivity can be directly extracted from the peak power. A sinusoidal vibration at 100 Hz is applied within the range of 1 g–4 g in the direction orthogonal to the resonator device (z-direction). As shown in Fig. 9, a spur is generated at offset frequency of 100 Hz from the carrier in the phase noise measurement results.

Using (3), the vibration sensitivity (Γ_z) is extracted to be less than 4 ppb/g (Fig. 10). This result is comparable with some SC-cut quartz-based oscillators. However, we believe that the vibration sensitivity is still dominated by the electrical components in the measurement setup [11], including bondwires, electrical connections, etc. The silica resonator itself should have significantly smaller vibration sensitivity.

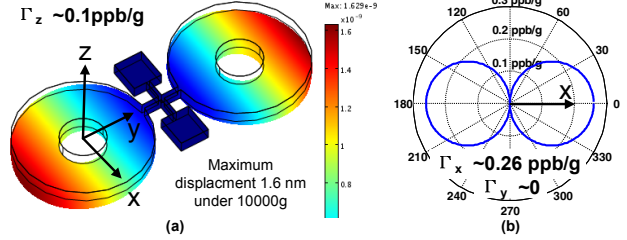


Figure 8: (a) Simulated bending due to 10000 g acceleration in z-direction and vibration sensitivity (Γ_z); (b) Simulated in-plane vibration sensitivity.

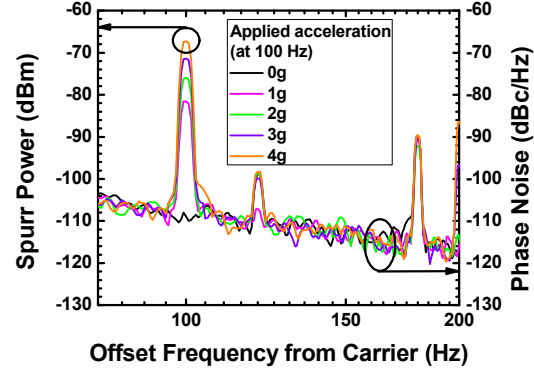


Figure 9: Phase noise measurement results of the silica MEMS oscillator, showing spurs in responses of sinusoidal vibration in the range of 1-4g at 100 Hz.

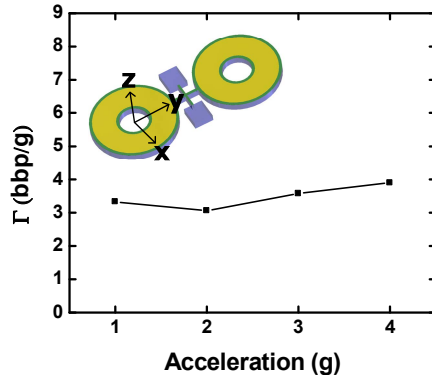


Figure 10: Extracted z-axis acceleration sensitivity of the silica MEMS oscillator.

OSCILLATOR FREQUENCY TUNING

While fused silica resonator is shown to have a small acoustic loss, the relatively large temperature coefficient of frequency (TCF) along with the vibration sensitivity of the oscillator calls for frequency tuning techniques. Specifically, the 4.9 MHz breathing mode has a measured first-order TCF of +90 ppm/ $^{\circ}\text{C}$ [8]. The low thermal conductivity of fused silica facilitates the implementation of ovenized MEMS resonator in a silica package, as discussed earlier. Frequency tuning techniques can be used to compensate for residual drift due to such small

temperature fluctuations inside the ovenized package, the vibration-induced frequency shift, or the frequency drift due to other environmental effects. For this purpose, two tuning mechanisms are discussed in this section: capacitive tuning and piezoelectric tuning.

Capacitive Frequency Tuning

Capacitors C_{p1} and C_{p2} in the Pierce oscillator (Fig. 5) can be changed to pull the silica MEMS oscillator frequency. To characterize the tuning characteristic, two Zetex 835A varactors are connected in parallel with fixed capacitors to form C_{p1} and C_{p2} . Fig. 11 plots the frequency shift of the silica oscillator when both C_{p1} and C_{p2} are changed by changing the DC voltage of the varactors. A change of 33 pF in both C_{p1} and C_{p2} causes 2 KHz (*i.e.* 408 ppm) of frequency shift in the oscillator output signal. The extracted pulling sensitivity is 1.4–3.7 ppm/pF. To achieve more accurate capacitive tuning and lower noise, varactors can be replaced by digital switched capacitor banks.

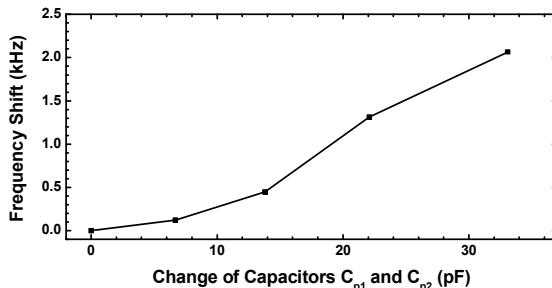


Figure 11. Measured oscillator output frequency shift as both capacitors C_{p1} , C_{p2} are changed.

Piezoelectric Frequency Tuning

By applying a DC bias voltage in addition to the AC signal to the top electrode, the resonance frequency can be tuned. Here the frequency tuning is a result of the stiffness change of the AlN layer with DC bias. Such piezoelectric tuning effect has been previously reported in a thickness-mode FBARs [12] and can be applied to the piezoelectric-on-silica resonator of this work. Fig. 12 shows the linear and bidirectional frequency shift of the oscillator with an applied bias in the range of ± 20 V. A piezoelectric tuning coefficient of -0.4 ppm/V is extracted from this measurement. The tuning coefficient (γ) is much smaller than that of FBARs [12], as applied DC bias only changes the stiffness of the thin-film AlN layer on top of a thick fused silica material. Such small tuning coefficient is suitable for high resolution tuning of the piezoelectric-on-silica timing reference.

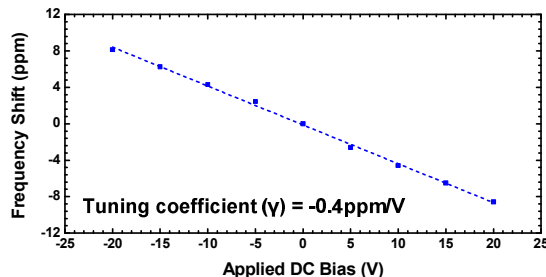


Figure 12: Measured fractional frequency shift versus piezoelectric tuning voltage.

CONCLUSION

In this work, a 4.9 MHz fused silica MEMS oscillator has been demonstrated using a CMOS driver amplifier circuit. The silica MEMS oscillator exhibits good phase-noise performance at a low-supply voltage. Two frequency tuning techniques have also been demonstrated, which can be used to compensate for the oscillator frequency drift and variations due to temperature or other environmental effects. Silica micro-resonators exhibit low vibration sensitivity, making them a good candidate for applications in dynamic platforms. These results show promise for silica MEMS oscillators in timing or resonant sensing applications.

ACKNOWLEDGEMENTS

This work was supported by DARPA under Single-chip Timing and Inertial Measurement Unit (TIMU) program, award #N66001-11-C-4170. The authors would like to acknowledge the staff at Michigan Lurie Nanofabrication Facilities (LNF).

REFERENCES

- [1] Y.-W. Lin, *et al.*, "Low phase noise array-composite micromechanical wine-glass disk oscillator," *Tech. Digest IEEE IEDM 2005*, Dec. 2005.
- [2] H. M. Lavasanian, *et al.*, "A 145MHz low phase-noise capacitive silicon micromechanical oscillator," *Tech. Digest IEEE IEDM 2008*, Dec. 2008.
- [3] H. M. Lavasanian, *et al.*, "A 500MHz Low Phase-Noise AlN-on-Silicon Reference Oscillator," *IEEE CICC 2007*, pp. 599-602, Sept. 2007.
- [4] H. Lee, *et al.*, "Low jitter and temperature stable MEMS oscillators," *Tech. Digest IEEE IFCS*, 2012.
- [5] G. K. Ho, *et al.*, "Temperature Compensated IBAR Reference Oscillators," *Proc. IEEE MEMS 2006*, pp. 910-913, 2006.
- [6] J. C. Salvia, *et al.*, "Real-time temperature compensation of MEMS oscillators using an integrated micro-oven and a phase-locked loop," *J. Microelectromech. Syst.*, pp. 192-201, Feb. 2010.
- [7] V. B. Braginskii, V. P. Mitrofanov, *Systems with Small Dissipation*, U. of Chicago Press, 1985.
- [8] Z. Wu, *et al.*, "Piezoelectrically transduced high- Q silica micro resonators", *Proc. IEEE MEMS 2013*, Jan. 2013.
- [9] D. B. Leeson, "A simple model of feedback oscillator noise spectrum," *Proceedings of IEEE*, vol. 54, no. 2, pp. 329-330, Feb. 1966.
- [10] R. L. Filler, "The acceleration sensitivity of quartz crystal oscillators: a review" *IEEE Trans. on UFFC*, pp. 297-305, 1988.
- [11] B. Kim, "Acceleration sensitivity of small-gap capacitive micromechanical resonator oscillators," *IEEE IFCS 2010*, pp. 273-278, June 2010.
- [12] W. Pang, *et al.*, "Electrical frequency tuning of film bulk acoustic resonator," *J. Microelectromech. Syst.*, vol. 16, no. 6, pp. 1303-1313, Dec. 2007.

CONTACT

*Z.Z. Wu, tel: +1-734-3899507; zzwu@umich.edu

*M. Rais-Zadeh; minar@umich.edu